SLAC-PUB-6618
August 1994
(T/E)

STUDIES OF STRONG ELECTROWEAK SYMMETRY BREAKING AT FUTURE e^+e^- LINEAR COLLIDERS *

TIMOTHY L. BARKLOW
Stanford Linear Accelerator Center
Stanford University, Stanford, California 94309

ABSTRACT

Methods of studying strong electroweak symmetry breaking at future e^+e^- linear colliders are reviewed. Specifically, we review precision measurements of triple gauge boson vertex parameters and the rescattering of longitudinal W bosons in the process $e^+e^- \to W^+W^-$. Quantitative estimates of the sensitivity of each technique to strong electroweak symmetry breaking are included.

1. Introduction

The exploration of electroweak symmetry breaking is the primary task of the next generation of pp and e^+e^- colliders. In this paper we review how strong electroweak symmetry breaking can be studied using the process $e^+e^- \to W^+W^-$ at the next generation e^+e^- linear collider (NLC). We assume two stages for the center-of-mass energy and luminosity of the NLC.[1] In the initial stage the center-of-mass energy is 500 GeV and the design luminosity is 0.8×10^{34} cm^{-1} s^{-1}. In the second stage the center-of-mass energy is 1500 GeV and the design luminosity is 1.9×10^{34} cm^{-1} s^{-1}. We will assume 10^7 seconds at the design luminosity for our integrated luminosity.

Strong electroweak symmetry breaking affects the reaction $e^+e^- \to W^+W^-$ by producing anomalous couplings at the $W^+W-\gamma$ and W^+W^-Z vertices and by producing observable W^+W^- final-state rescattering effects. We will use the three-gauge boson vertex formalism of Ref. 2 when we discuss anomalous three-gauge boson couplings. For example, we will be referring later to the parameters κ_γ, κ_Z, and g_1^Z, which are defined in Eq. 2.1 of Ref. 2.

*Work supported by Department of Energy contract DE-AC03-76SF00515.

Presented at the DPF '94 Conference: 1994 Meeting of the Division of Particles and Fields of the APS, Albuquerque, NM, August 2-6, 1994

Final-state rescattering in $e^+e^- \to W^+W^-$ provides information about the $J = 1$ partial wave in the scattering process $W_L^+W_L^- \to W_L^+W_L^-$.[3] In particular, it is quite sensitive to a vector resonance. Final-state rescattering is incorporated by multiplying the standard model amplitude for $e^+e^- \to W_L^+W_L^-$ by the complex-form factor F_T, where

$$F_T = \exp[\frac{1}{\pi}\int_0^\infty ds'\delta(s', M_\rho, \Gamma_\rho)\{\frac{1}{s'-s-i\epsilon} - \frac{1}{s'}\}], \quad (1)$$

$$\delta(s) = \frac{1}{96\pi}\frac{s}{v^2} + \frac{3\pi}{8}\left[tanh(\frac{s-M_\rho^2}{M_\rho\Gamma_\rho}) + 1\right], \quad (2)$$

$v = 240$ GeV, M_ρ is the techni-rho mass and Γ_ρ is the techni-rho width. Note that for an infinite techni-rho mass $\delta(s)$ becomes

$$\delta(s) = \frac{1}{96\pi}\frac{s}{v^2}, \quad (3)$$

reflecting the low-energy theorem (LET) amplitude for longitudinal gauge boson scattering.

We use the chiral Lagrangian formalism[4] for the description of strong electroweak symmetry breaking. The electroweak symmetry breaking Lagrangian $\mathcal{L}_{SB}$ is given by

$$\mathcal{L}_{SB} = \mathcal{L}^{(2)} + \mathcal{L}^{(4)} + \cdots + \mathcal{L}^{(res)} + \cdots, \quad (4)$$

where $\mathcal{L}^{(2)}$ and $\mathcal{L}^{(4)}$ are defined in Eq. 2.4 and Eq. 2.5 of Ref. 4, and $\mathcal{L}^{(res)}$ represents the Lagrangian for TeV-scale scalar or vector resonances. The terms in $\mathcal{L}^{(4)}$ with coefficients L_{9L} and L_{9R} produce the following anomalous three-gauge boson couplings:

$$\kappa_\gamma = 1 + \frac{e^2}{32\pi^2 s_w^2}(L_{9L} + L_{9R}) \quad (5)$$

$$\kappa_Z = 1 + \frac{e^2}{32\pi^2 s_w^2}(L_{9L} - \frac{s_w^2}{c_w^2}L_{9R}) \quad (6)$$

$$g_1^Z = 1 + \frac{e^2}{32\pi^2 s_w^2}\frac{L_{9L}}{c_w^2}, \quad (7)$$

where $s_w^2 = \sin^2\theta_w$ and $c_w^2 = \cos^2\theta_w$.

2. Analysis of W^+W^- Final State

We perform a final-state helicity analysis of $e^+e^- \to W^+W^-$ in order to obtain the greatest sensitivity to anomalous three-gauge boson couplings and $W_L^+W_L^-$ rescattering. The final-state topology with one W decaying to an electron or muon (plus neutrino), and the other decaying hadronically is best for such an analysis. Other event topologies will not be considered.

The W^- production angle Θ is defined to be the angle between the initial state e^- and the W^- in the e^+e^- rest frame. We define θ^* and ϕ^* to be the polar and azimuthal angles of the lepton in the rest frame of the W that decays leptonically. Let $\overline{\theta}^*$ and

$\overline{\phi}^*$ denote the polar and azimuthal angles of the quark jets in the rest frame of the W that decays hadronically. We assume no quark flavor tagging, and so we must average over the two quark directions.

The five measured variables that we use in our maximum likelikhood fits are $\cos\Theta, \cos\theta^*, \phi^*, \cos\overline{\theta}^*$, and $\overline{\phi}^*$. They are reconstructed from detected quantites such as the energies and angles of the lepton and the quark jets.

Only two cuts are imposed. First, we require that $|\cos\Theta| < 0.8$ in order to ensure that the event is well within the detector volume. The second cut forces the W^+W^- invariant mass to be within a few GeV of the nominal e^+e^- center-of-mass energy, and forces the W^+ and W^- invariant masses to each be within a few GeV of the W pole mass. In order to impose the second cut we reconstruct the mass of the leptonically decaying W (M_{W_1}) and the mass of the hadronically decaying W (M_{W_2}). The variable M_{W_2} is reconstructed by imposing four energy-momentum constraints and solving for the four unknowns $\{\vec{P}_\nu,\ M_{W_2}\}$, where $\vec{P}_\nu$ is the momentum of the neutrino from the leptonically decaying W. Then M_{W_1} is

$$M_{W_1} = \left[(E_l + E_\nu)^2 - (\vec{P}_l + \vec{P}_\nu)^2\right]^{1/2} . \tag{8}$$

Define

$$\chi^2 \equiv \frac{(M_{W_1} - M_W)^2}{\Gamma_W^2} + \frac{(M_{W_2} - M_W)^2}{\Gamma_W^2} . \tag{9}$$

Our second cut is then

$$\chi^2 < 2 . \tag{10}$$

3. Maximum Likelihood Formalism

We use the maximum likelihood method to fit for L_{9L}, L_{9R}, or for the real and imaginary parts of F_T. Our maximum likelihood function L is given by

$$L = \prod_1^N f(\vec{x}_i, \vec{a}) , \tag{11}$$

where N is the number of events, f is the probability density function, $\vec{x}_i$ are the measured variables $\vec{x}$ for event i, and $\vec{a}$ are the fit parameters. The probability density function is normalized to unity:

$$\int d\vec{x}\ f(\vec{x}, \vec{a}) = 1 . \tag{12}$$

The measured variables $\vec{x}$ are $\vec{x} = (\cos\Theta, \cos\theta^*, \phi^*, \cos\overline{\theta}^*, \overline{\phi}^*)$. The fit parameters are $\vec{a} = (L_{9L}, L_{9R})$ or $\vec{a} = (Re(F_T), Im(F_T))$. The covariance matrix V for the $\vec{a}$ that maximizes L is given by

$$(V^{-1})_{ij} = N\int d\vec{x}\ \frac{1}{f}\Big(\frac{\partial f}{\partial a_i}\Big)\Big(\frac{\partial f}{\partial a_j}\Big) . \tag{13}$$

If we have an unnormalized probability density function $\mu(\vec{x}, \vec{a})$ then we write

$$f = \frac{\mu}{\Xi}, \quad \Xi(\vec{a}) = \int d\vec{x}\ \mu(\vec{x}, \vec{a}) . \tag{14}$$

In order to account for detector resolution, experimental cuts, initial-state radiation, initial-state electron polarization, and distinct final-state event topologies, we use the following expression for the unnormalized probability density function μ:

$$\mu_{kl}(\vec{x}_l, \vec{a}) = \int d\vec{x}_l'\ d\vec{q}_l\ d\vec{z}\ r_l(\vec{x}_l, \vec{x}_l', \vec{q}_l, \vec{z}\,)\eta_l(\vec{x}_l', \vec{q}_l, \vec{z}\,)t_{kl}(\vec{x}_l', \vec{q}_l, \vec{z}\,, \vec{a})h_l(\vec{z}\,) , \tag{15}$$

where k is the initial-state electron polarization index and l is the final-state event topology index. Here $\vec{x}'$ denotes the true values of the measured variables, and $\vec{q} = (q^2, \overline{q}^2)$, where q^2 and $\overline{q}^2$ are the invariant masses squared of the leptonically decaying W and hadronically decaying W respectively. We define $\vec{z} = (z_1, z_2)$ where $z_1 = E_{e^-}/E_b$, $z_2 = E_{e^+}/E_b$, E_b is the beam energy, and $E_{e^\pm}$ are the electron and positron energies following initial state bremsstrahlung and beamstrahlung. The resolution function is $r(\vec{x}, \vec{x}', \vec{q}, \vec{z}\,)$, $\eta(\vec{x}', \vec{q}, \vec{z}\,)$ is the detection efficiency function, $t(\vec{x}', \vec{q}, \vec{z}\,, \vec{a})$ is the multi-differential cross-section, and $h(\vec{z}\,)$ is the multi-differential luminosity.

With initial-state polarizations and distinct final-state event topologies, the expression for $(V^{-1})_{ij}$ is somewhat complicated unless we make some additional defintions. Define

$$\Xi_{kl}(\vec{a}) = \int d\vec{x}_l\ \mu_{kl}(\vec{x}_l, \vec{a}) \tag{16}$$

and

$$\lambda_k = \frac{\mathcal{L}_k}{\mathcal{L}} , \tag{17}$$

where $\mathcal{L}_k$ is the luminosity at polarization k and $\mathcal{L}$ is the total luminosity. Note that the systematic error for λ_k will be much smaller than the systematic error for $\mathcal{L}_k$. Next define

$$\Lambda(\vec{a}) = \sum_{k,l} \lambda_k \Xi_{kl} \tag{18}$$

$$\alpha_{kl}(\vec{a}) = \frac{\lambda_k \Xi_{kl}}{\Lambda} \tag{19}$$

$$\zeta_{ikl}(\vec{a}) = \frac{1}{\Xi_{kl}}\frac{\partial \Xi_{kl}}{\partial a_i} - \frac{1}{\Lambda}\frac{\partial \Lambda}{\partial a_i} \tag{20}$$

$$\psi_{ikl}(\vec{x}_l, \vec{a}) = \frac{1}{\mu_{kl}}\frac{\partial \mu_{kl}}{\partial a_i} - \frac{1}{\Xi_{kl}}\frac{\partial \Xi_{kl}}{\partial a_i} \tag{21}$$

$$\omega_{ijl}(\vec{x}_l, \vec{a}) = \frac{1}{\Lambda}\sum_k \lambda_k \mu_{kl}\psi_{ikl}\psi_{jkl} . \tag{22}$$

The inverse of the covariance matrix is then given by

$$(V^{-1})_{ij} = N\sum_l \left[\Phi_{ijl} + \Omega_{ijl}\right] \tag{23}$$

where

$$\Phi_{ijl} = \sum_k \alpha_{kl}\zeta_{ikl}\zeta_{jkl} \quad (24)$$

$$\Omega_{ijl} = \int d\vec{x}_l \, \omega_{ijl} \quad . \quad (25)$$

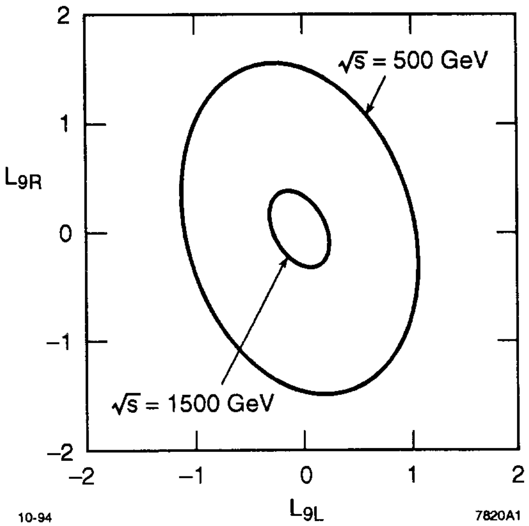

Fig. 1. The 95% confidence level contours for L_{9L} and L_{9R} at $\sqrt{s} = 500$ GeV with 80 fb^{-1}, and at $\sqrt{s} = 1500$ GeV with 190 fb^{-1}. The outer contour is for $\sqrt{s} = 500$ GeV. In each case the initial state electron polarization is 90%.

4. Results

We will now plot 95% confidence level contours for some fit parameters based on the covariance matrix calculation described above. In making these plots our expression for $\mu_{kl}(\vec{x}_l, \vec{a})$ has been simplified. The errors on our reconstructed quantities $\cos\Theta, \cos\theta^*, \phi^*, \cos\overline{\theta}^*, \overline{\phi}^*$ are small enough that the resolution function r_l can be approximated by a delta function. Also, the imposition of our second cut, Eq. 10, allows us to approximate the efficiency function η_l by a delta function at $q^2 = M_W^2$, $\overline{q}^2 = M_W^2$, $z_1 = 1$, and $z_2 = 1$. As a result, we have

$$\mu_{kl}(\vec{x}_l, \vec{a}) = t_{kl}(\vec{x}_l, \vec{a}) \quad (26)$$

where $t_{kl}(\vec{x}_l, \vec{a})$ is now the narrow-width, multi-differential cross-section[2] with initial-state electron polarization $P_e(k)$ at the nominal e^+e^- center-of-mass energy. For all of our examples we will assume that half of the luminosity is taken with $P_e(1) = -0.9$ and half with $P_e(2) = +0.9$. The final-state event topology index takes on the values $l = 1, 2$, where $l = 1$ refers to the final state with the W^- decaying leptonically and the W^+ decaying hadronically, while $l = 2$ refers to the final state with the W^- decaying hadronically and the W^+ decaying leptonically.

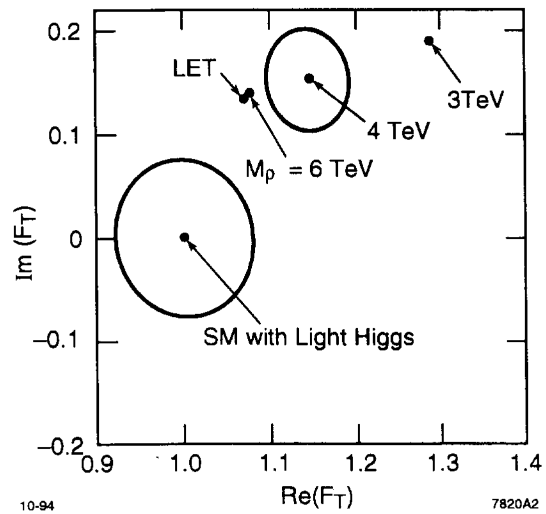

Figure 2. Confidence level contours for the real and imaginary parts of F_T at $\sqrt{s} = 1500$ GeV with 190 fb^{-1}. The initial state electron polarization is 90%. The contour about the light Higgs value of $F_T = (1, 0)$ is 95% confidence level and the contour about the $M_\rho = 4$ TeV point is 68% confidence level.

Figure 1 shows the 95% confidence level contours for L_{9L} and L_{9R} at $\sqrt{s} = 500$ GeV with 80 fb^{-1}, and at $\sqrt{s} = 1500$ GeV with 190 fb^{-1}. The outer contour is for $\sqrt{s} = 500$ GeV.

Figure 2 contains confidence level contours for the real and imaginary parts of F_T at $\sqrt{s} = 1500$ GeV with 190 fb^{-1}. Shown are the 95% confidence level contour about the light Higgs value of F_T, and the 68% confidence level (i.e., 1σ probability) contour about the value of F_T for a 4 TeV techni-rho. We see that even the non-resonant LET point is well outside the light Higgs 95% confidence level region. In fact, the LET point intersects the 99.99945% confidence level contour about the light Higgs point, corresponding to a 4.5σ signal. The 6 TeV and 4 TeV techni-rho points correspond to 4.8σ and 6.5σ signals, respectively. At a slightly higher integrated luminosity of 225 fb^{-1}, we would obtain 7.1σ, 5.3σ and 5.0σ signals for a 4 TeV techni-rho, a 6 TeV techni-rho, and LET, respectively.

In conclusion, the process $e^+e^- \to W^+W^-$ is an effective probe of strong electroweak symmetry breaking. The chiral Lagrangian parameters L_{9L} and L_{9R} can be determined with an accuracy of ± 1.5 at $\sqrt{s} = 500$ GeV and ± 0.5 at $\sqrt{s} = 1500$ GeV (95% C.L.). $W_L^+ W_L^-$ rescattering allows us to discover and identify techni-rho resonances with masses as large as 4 TeV. For higher techni-rho masses it may be difficult to distinguish the resonances from LET, but the higher mass techni-rho's, as well as LET, can be clearly distinguished from the Standard Model with a light Higgs.

References

1. R. Ruth (private communication).
2. K. Hagiwara, R.D. Peccei, D. Zeppenfeld, and K. Hikasa, *Nucl. Phys.* **B282** (1987) 253.
3. M.E.Peskin, in *Physics in Collision 4*, ed. A.Seiden (Editions Frontieres, Gif-sur-Yvette, 1984).
4. J. Bagger, S. Dawson, and G. Valencia, *Nucl. Phys.* **B399** (1993) 364.